TÜBİTAK

Turkish Journal of Chemistry

http://journals.tubitak.gov.tr/chem/

Research Article

Turk J Chem
(2018) 42: 1611 – 1622
© TÜBİTAK
doi:10.3906/kim-1804-33

Metal nanoparticles/carbon nanotube modified electrodes for voltammetric determination of boron

Lokman LİV[1], **Zekerya DURSUN**[2], **Nuri NAKİBOĞLU**[1,3,*]

[1]Electrochemistry Laboratory, Chemistry Group, TÜBİTAK National Metrology Institute (TÜBİTAK UME), Kocaeli, Turkey

[2]Department of Chemistry, Faculty of Science, Ege University, İzmir, Turkey

[3]Department of Chemistry, Faculty of Arts and Sciences, Balıkesir University, Balıkesir, Turkey

Received: 17.04.2018 • **Accepted/Published Online:** 22.07.2018 • **Final Version:** 06.12.2018

Abstract: This study describes a sensitive and accurate voltammetric method for determination of boron using metal nanoparticles/carbon nanotube modified electrodes. The oxidation peak of Alizarin Red S (ARS) at –0.59 V in the boron-ARS complex formed in ammonium/ammonia buffer solution (pH 8.5) was evaluated as a response. The electrode modification conditions and experimental parameters affecting the peak height were optimized. The characteristics of modified electrodes were investigated using cyclic voltammetry, electrochemical impedance spectroscopy, scanning electron microscope, energy dispersive X-ray spectroscopy, high resolution transmission electron microscopy, and X-ray photoelectron spectroscopy. The limits of detection ($3s_{y/x}$) and the analytical ranges for gold nanoparticles/carbon nanotube modified electrode (AuNP/CNT/GCE) and copper nanoparticles/carbon nanotube modified electrode (CuNP/CNT/GCE) for 40 s accumulation times were 55 μg L^{-1} and 83 μg L^{-1} and 182–1500 μg L^{-1} and 278–1000 μg L^{-1}, respectively. The method was applied to various water and eye drop samples. The results obtained for two modified electrodes were compared with inductively coupled plasma-mass spectrometry results and there was no statistically significant difference between the methods at 95% confidence level. Moreover, UME CRM 1201 (Elements in Spring Water) was used for the accuracy check of the proposed method.

Key words: Boron, Alizarin Red S, nanoparticles, modified electrode, carbon nanotubes, voltammetry

1. Introduction

Boron and its compounds are prevalently found in nature and have been used in many fields such as glass, medicine, farm, cleaning, nuclear, and energy production industries due to their good features. Additionally, boric acid and sodium borate have been used in some eye drops due to effectiveness against fungal and bacterial infections. Boron is important for human health due to providing calcium, magnesium, and phosphorus regulation and it has a supporting effect for bone growth.[1] It is also very important and essential in tiny doses for growth in plants and animals.[2] Boron is mostly found as boric acid (H_3BO_3) in acidic water samples and tetrahydroxymetaborate ($B(OH)_4^-$) is the primary species at higher than pH 10.[3] The EPA[4] and WHO[5] released the limit values for boron in drinking water as 1.4 mg L^{-1} and 2.4 mg L^{-1}, respectively.

Voltammetric methods have some good features such as simplicity, cheapness, rapidity, and sensitivity. Therefore, researchers have shown considerable interest in voltammetry for determination of boron in recent

*Correspondence: nnuri@balikesir.edu.tr

years. It is well known that boric acid and its pH-dependent species are not electroactive in the potential range of the working electrode. For this reason, an electroactive chemical reagent that is able to form a complex with boron has been generally used for voltammetric determination of boron. Voltammetric methods using a poly xylenol orange modified pencil graphite electrode,[1] pencil graphite electrode,[3] dropping mercury electrode,[6–9] hanging mercury electrode,[10–15] glassy carbon electrode,[16] and cobalt phthalocyanine modified carbon paste electrode[17] have been reported. The existing voltammetric methods for determination of boron including the used techniques and electrodes, media, and their limits of detection and analytical ranges were discussed and summarized in our previous studies.[1,3] In particular, in methods in which solid working electrodes are used, the main problem is that the oxidation peaks of the free ligand and the ligand in the boron-ligand complex cannot be precisely separated from each other. This situation, which makes it difficult to accurately measure peak currents, is clearly observed in the existing studies.[1,3,16] Therefore, new electrode materials are needed to overcome this problem.

The aim of the present study was to develop an alternative voltammetric method using metal nanoparticles/carbon nanotube modified electrodes (MNP/CNT/GCEs) for determination of boron in real samples. For this purpose, the oxidation peak of Alizarin Red S (ARS) in the boron-ARS complex formed in ammonium/ammonia buffer solution (pH 8.5) at MNP/CNT/GCEs was evaluated as a response. To our knowledge, this is the first time that MNP/CNT/GCEs are used for voltammetric determination of boron in real samples. The parameters for preparation of modified electrodes such as concentration of gold and copper solutions, sulfuric acid concentration, cycle number, and scan rate were optimized. Additionally, chemical and instrumental parameters such as pH, type and concentration of supporting electrolyte, ARS concentration, ionic strength, interval time, step and pulse amplitude, pulse time, and accumulation potential and time were investigated. The method was applied to various water and eye drop samples. The results were compared with those obtained from the inductively coupled plasma-mass spectrometry (ICP-MS) method. Furthermore, a certified reference material (UME CRM 1201: Elements in Spring Water) was used for the accuracy check of the proposed method.

2. Results and discussion

2.1. Characterization of modified electrodes

Cyclic voltammetry (CV) was used for modification of the electrode with gold and copper nanoparticles. The expected anodic (at 1.12 V for gold, at 0.01 V and 0.38 V for copper) and cathodic (at 0.54 V for gold, at –0.07 V and –0.45 V for copper) peaks indicating the modification of the electrode were observed. The optimum conditions for gold modification were found to be 5×10^{-5} M $HAuCl_4$, 0.25 M H_2SO_4, 50 mV s^{-1} scan rate, and 4 cycle number. Similarly, optimum conditions for copper modification were found to be 5×10^{-5} M $CuSO_4$, 0.15 M H_2SO_4, 50 mV s^{-1} and 4 cycle number.

After completing the electrode preparation procedure, CV voltammograms were recorded for each electrode glassy carbon electrode (GCE), carbon nanotube (CNT) modified glassy carbon electrode (CNT/GCE), copper nanoparticles/carbon nanotube modified electrode (CuNP/CNT/GCE), and gold nanoparticles/carbon nanotube modified electrode (AuNP/CNT/GCE) in 5 mM $K_4Fe(CN)_6$ solution containing 0.1 M KNO_3. GCE showed the lowest peak current. Anodic and cathodic peaks increased regularly in the case of CNT/GCE, CuNP/CNT/GCE, and AuNP/CNT/GCE, respectively. These results also indicated that the electrodes were successfully modified.

For the further investigation, scanning electron microscope (SEM) images of CNT/GCE, CuNP/CNT/GCE, and AuNP/CNT/GCE were taken. CNTs are almost homogeneously distributed on the GCE (Figure 1). The H_2SO_4 activated CNTs are formed as a network with various densities and contain some remaining impurities, shiny and sticky shapes from the activation procedure. On the other hand, the presence of copper and gold nanoparticles on the CNT/GCE is not clearly observed (not shown here), because the metal ion concentrations were used as dilute concentrations during the electrochemical deposition.

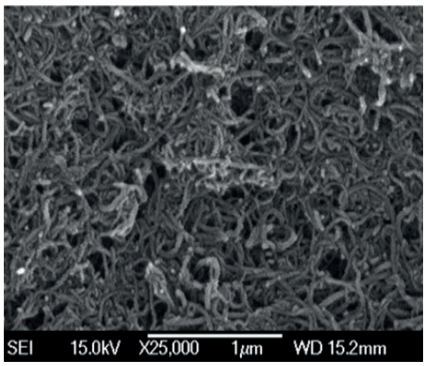

Figure 1. SEM image of CNT/GCE.

The observed copper and gold metal nanoparticles appear to have a narrow size distribution, fairly visible as spherical shapes of metal nanoparticles (MNPs) at the end of multiwalled carbon nanotubes (MWCNTs), which confirms that all formed copper and gold nanoparticles are attached to the nanotubes. The presence of both metals on the CuNP/CNT/GCE and AuNP/CNT/GCE surfaces is revealed by energy dispersive X-ray spectroscopy (EDX) studies (Figure 2).

Representative high resolution transmission electron microscopy (HRTEM) images of the copper and gold nanoparticles are fairly homogeneously distributed on the MWCNTs in Figure 3. The cloudy and threaded structures show the CNTs as blackish-grayish and roughly spherical with some triangular-shaped, in diameters ranging from 8.57 to 28.48 nm for copper and in diameters ranging from 19.25 to 42.14 nm for gold nanoparticles on these structures.

X-ray photoelectron spectroscopy (XPS) was used to evaluate the surface composition, chemical oxidation states, and electronic configuration of MWCNTs, Cu, and Au on modified electrode surfaces. Figure 4 reveals the XPS survey spectra of CuNP/CNT/GCE and AuNP/CNT/GCE. The C 1s core level spectrum is displayed in Figures 4A and 4B. The main peak at 284.48 eV corresponds to C–C and C=C bonds attributed to MWCNTs and a shoulder signal at 288.28 eV could be attributed to C=O. The C=O bond on the MWCNTs was formed during the activation or electrochemical deposition of metal particles on the electrode surface. The presence of oxygen on the surface was also proved by monitoring the peaks at 531.58 eV and 532.68 eV for CuNP/CNT/GCE (Figure 4A′) and 532.68 eV, 532.98 eV, and 533.38 eV for AuNP/CNT/GCE (Figure 4B′). On the other hand, the presence of metal or metal oxide particles on the modified electrodes is shown in Figures 4A″ and 4B″. For Figure 4A″ the Cu $2p_{3/2}$ photoelectron peak was obtained, resolving it into three peaks. The binding energy of the highest intensities were observed at 932.48 eV and 952.68 eV, corresponding to metallic Cu or Cu_2O. In addition, the Cu $2p_{3/2}$ XPS spectra proved that the copper surface is covered mainly by cupric CuO, as indicated by the shake-up satellite structure, centered at a binding energy of 944.18 eV. Figure 4B″ shows the Au 4f spectrum resolved into two spin-orbit components (Au $4f_{7/2}$ and $4f_{5/2}$) on AuNP/CNT/GCE. As

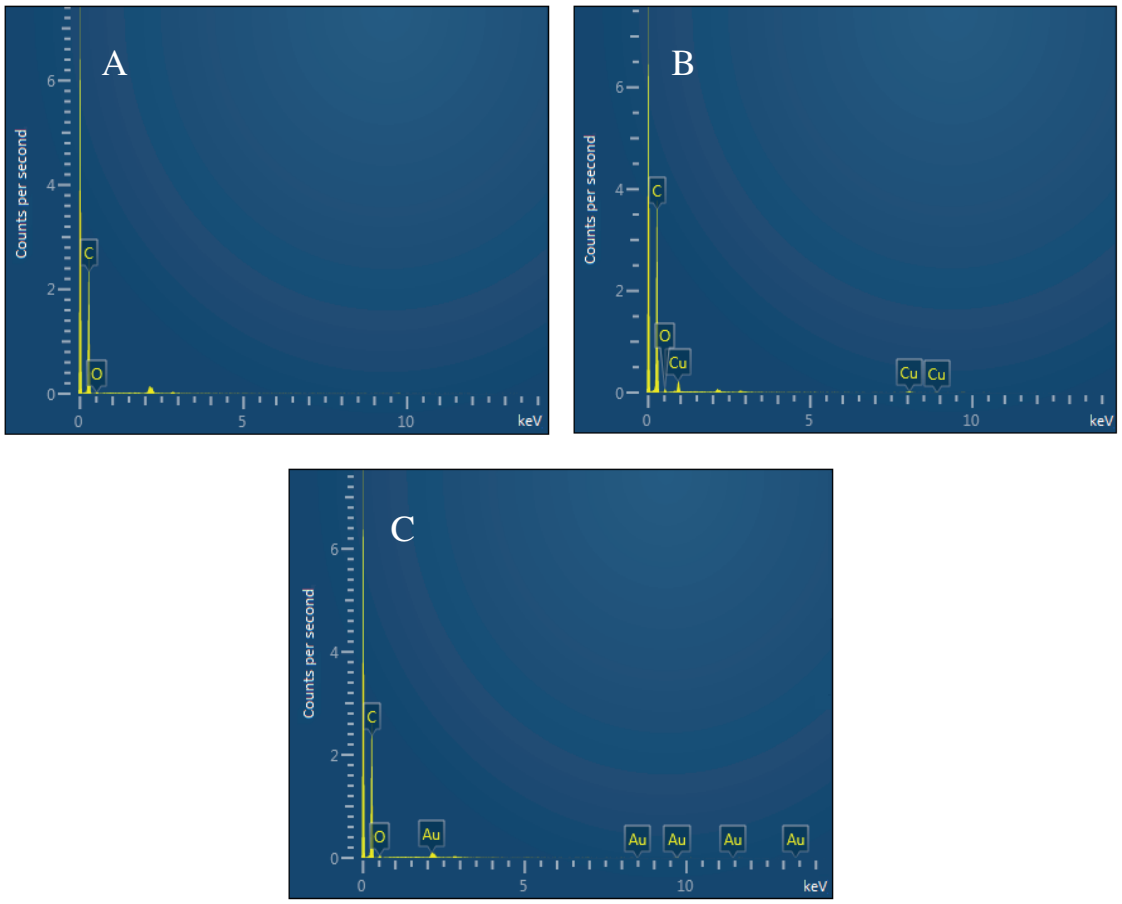

Figure 2. EDX spectra of CNT/GCE (A), CuNP/CNT/GCE (B), and AuNP/CNT/GCE (C).

shown in Figure 4B″, the Au $4f_{7/2}$ and Au $4f_{5/2}$ peaks formed at 84.08 and 87.71 eV, respectively, which are associated with metallic Au.

Electrochemical impedance spectra were recorded in the frequency ranges from 0.25 Hz to 50000 Hz for bare GCE, CNT/GCE, CuNP/CNT/GCE, and Au/CNT/GCE in the presence of 5.0 mM $K_3[Fe(CN)_6]/K_4[Fe(CN)_6]$ containing 0.1 M KNO_3 solution (figure not shown here). All electrodes have almost semicircular and linear portions. The almost semicircle corresponds to the charge transfer process at high frequencies, whereas linear portions correspond to the diffusion process at low frequencies for GCE and modified electrodes. The diameter of the semicircle shows the magnitude of electron-transfer resistance at the electrode surface. The obtained electrochemical impedance spectroscopy (EIS) data were fitted with an equivalent R(RC) circuit, which consists of the ohmic resistance of the electrolyte solution (R_s), the double layer capacitance (C_{dl}), and electron-transfer resistance (R_{ct}), which represents the diffusion of ions from the bulk of the electrolyte to the interface. The R_{ct} for the bare GCE was 669 Ω, which was higher than the R_{ct} values obtained for CNT/GCE (29.03 Ω). The R_{ct} values of CuNP/CNT/GCE and Au/CNT/GCE were 13.64 and 8.52 Ω, respectively. These data indicated the excellent electroconductibility of CuNP/CNT/GCE and Au/CNT/GCE surfaces. The lowest R_{ct} value for Au/CNT/GCE implies that the charge transfer process was relatively faster than those of the other electrodes used.

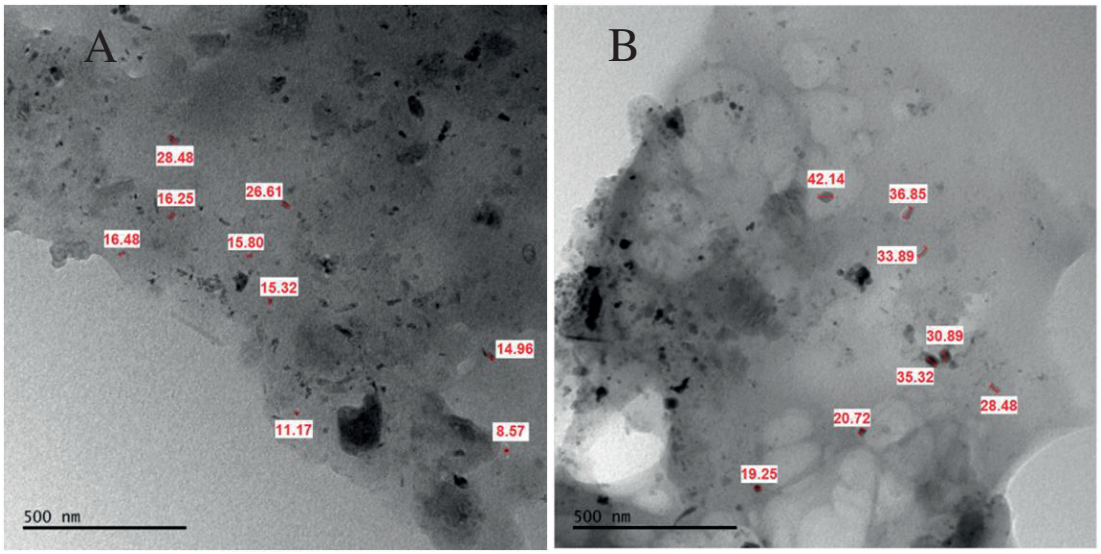

Figure 3. HRTEM images of CuNP/CNT/GCE (A) and AuNP/CNT/GCE (B).

2.2. Voltammetric behavior of boron-ARS complex at the modified electrodes

The differential pulse (DP) voltammograms obtained for both AuNP/CNT/GCE and CuNP/CNT/GCE in the absence and presence of 0.5 mg L^{-1} boron in solution containing 0.07 mM ARS and ammonium/ammonia buffer at pH 8.5 are shown in Figure 5A. The peaks of free ARS were obtained at –0.690 V for AuNP/CNT/GCE (Figure 5A-a) and –0.665 V for CuNP/CNT/GCE (Figure 5A-c), respectively. After addition of 0.5 mg L^{-1} boron, a well-defined oxidation peak belonging to the B-ARS complex showed up at –0.590 V for AuNP/CNT/GCE (Figure 5A-b) and at –0.570 V for CuNP/CNT/GCE (Figure 5A-d). The B-ARS system has previously been used for determination of boron at hanging mercury drop electrode[15] and cobalt phthalocyanine modified carbon paste electrode.[17] However, the B-ARS peak was not fully separated from the free ARS peak, particularly at the cobalt phthalocyanine modified carbon paste electrode. Obtaining a well-defined oxidation peak for B-ARS is the main advantage of AuNP/CNT/GCE or CuNP/CNT/GCE usage. Additionally, CV voltammograms at 50 mV s^{-1} scan rate were recorded for both modified electrodes in the absence (Figure 5B-a, c) and presence (Figure 5B-b, d) of 10 mg L^{-1} boron in solution containing 0.07 mM ARS and ammonium/ammonia buffer at pH 8.5. It is clear that the peak height obtained from AuNP/CNT/GCE is higher than that obtained from CuNP/CNT/GCE in both cases and the peak potentials were almost the same for both modified electrodes. Moreover, the CV voltammograms were scanned at 5, 10, 25, 50, 75, 100, 150, 200, 250, 300, 350, and 400 mV s^{-1} scan rates to explain the behavior of the B-ARS complex. The equation obtained from the logarithm of peak height versus logarithm of scan rate was $\log(I_{pc}) = 0.9521\ (\upsilon) + 0.3648$ ($R^2 = 0.998$), indicating an adsorption-controlled process, because the slope of the equation is very close to 1.

2.3. Optimization of the solution and instrumental parameters

Solution parameters such as pH, type and concentration of supporting electrolyte, ionic strength, and ARS concentration were optimized because they affect the boron-ARS complex formation and anodic oxidation of the complex. The pH effect was evaluated by recording DP voltammograms in the pH range of 6.5–9.0 with

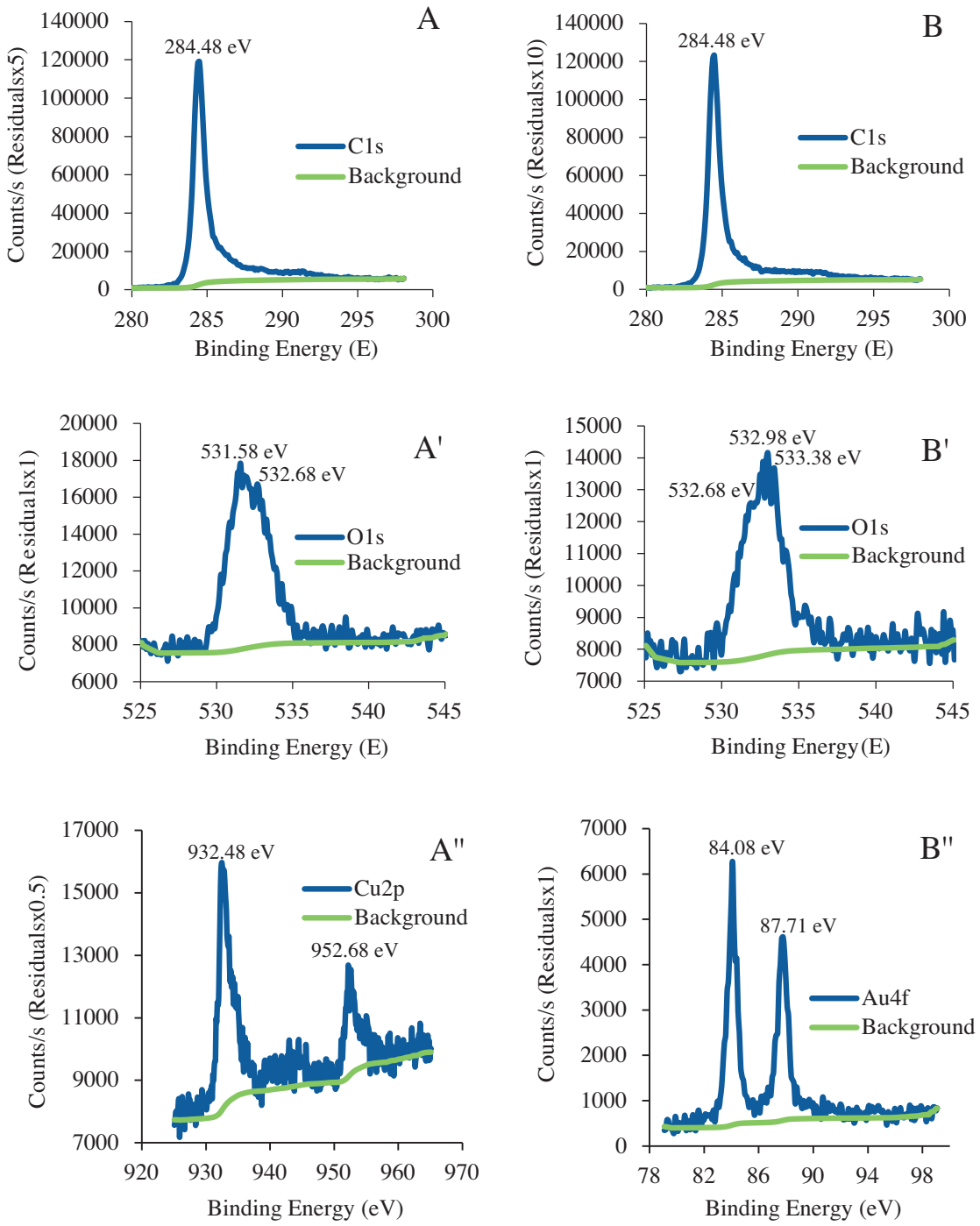

Figure 4. XPS spectra of CuNP/CNT/GCE (A, A′, and A″) and AuNP/CNT/GCE (B, B′, and B″).

0.5 pH unit increments in 0.5 M buffer solutions containing 0.07 mM ARS, 0.1 M KCl, and 0.5 mg L^{-1} boron. Phosphate buffer was used for the pH range between 6.5 and 8.0 and ammonium/ammonia buffer was used for pH between 8.5 and 9.0. No significant peak depending on boron concentration was observed at pH levels below 6.5. The plotted current-pH graph (not shown here) showed that the peak height conspicuously increased

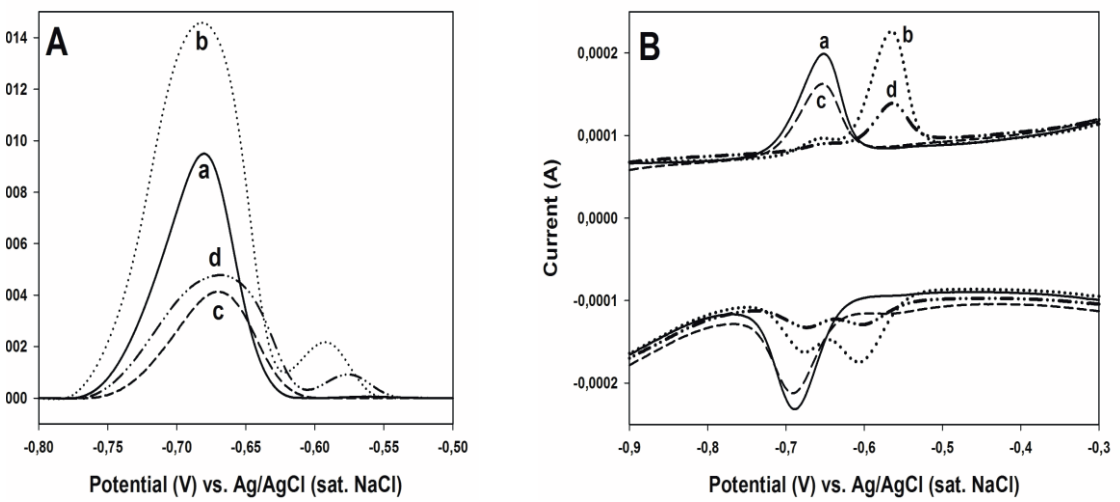

Figure 5. (A) DP voltammograms of ARS in the absence (a, c) and presence (b, d) of 0.5 mg L^{-1} boron in pH 8.5 NH_4^+/NH_3 buffer solution at AuNP/CNT/GCE (a, b) and CuNP/CNT/GCE (c, d). (B) Cyclic voltammograms of ARS in the absence (a, c) and presence (b, d) of 10 mg L^{-1} boron in pH 8.5 NH_4^+/NH_3 buffer solution at AuNP/CNT/GCE (a, b) and CuNP/CNT/GCE (c, d).

from pH 7.5 to 8.5 and then dramatically decreased. Therefore, the optimum pH value was chosen as 8.5. Afterwards, the concentration of the selected buffer solution was investigated in the range of 0.025–0.600 M. The peak height increased with increasing concentration of buffer solution and remained constant after 0.5 M. The concentration of NH_4^+/NH_3 buffer was selected as 0.5 M. Additionally, the pH-peak potential curve was drawn and the slope of this curve was –56.184 mV. This value is very close to ±59 mV, which depicts that the electrode reaction is realized with equal numbers of protons and electrons.

The effect of ionic strength on anodic peak height of the B-ARS complex was also investigated. The results obtained showed that the peak height was slightly increased up to 0.1 M KCl and decreased considerably after 0.2 M KCl. Therefore, the optimal concentration of KCl was chosen as 0.1 M. The ARS concentration is important for formation of the B-ARS complex and it affects the peak height. DP voltammograms were recorded in various ARS concentrations to find out the effect of ARS concentration on peak height (conditions: 0.5 M NH_4^+/NH_3, pH 8.5, 0.1 M KCl, 0.5 mg L^{-1} boron, scan rate: 3.6 mV s^{-1}, pulse amplitude: 70 mV, E_{acc}: –900 mV, $t_{acc.}$: 40 s). The plotted peak height-ARS concentration graph showed that the peak height increased up to 0.15 mM then almost remained constant. The concentration of ARS was selected as 0.07 mM because higher concentrations caused an increase in background current and asymmetrical B-ARS peaks.

Instrumental parameters such as interval time, step and pulse amplitude, pulse time, and accumulation potential and time were optimized as these parameters affect the anodic oxidation of the B-ARS complex. Step amplitude and interval time, which determine the scan rate, were optimized as 1 mV and 0.275 s, respectively. Consequently, the scan rate was calculated as 3.6 mV s^{-1}. Pulse amplitude and pulse time, accumulation potential, and accumulation time were optimized as 70 mV, 0.05 s, –900 mV, and 40 s, respectively.

2.4. Validation and application of the proposed method to real samples

The voltammograms were recorded under the optimum conditions for both AuNP/CNT/GCE (Figure 6A) and CuNP/CNT/GCE (Figure 6B). The obtained calibration graphs and equations are given next to these. The

limits of detection ($3s_{y/x}$) and the analytical ranges for AuNP/CNT/GCE and CuNP/CNT/GCE for 40 s accumulation times were 55 μg L^{-1} and 83 μg L^{-1} and 182–1500 μg L^{-1} and 278–1000 μg L^{-1}, respectively. The relative standard deviation values were found to be 2.14%, 2.38%, 2.57%, and 2.99% for 0.4, 0.7, 1.0, and 1.5 mg L^{-1} boron concentration levels for AuNP/CNT/GCE and 6.43%, 2.14%, and 5.56% for 0.2, 0.5, and 0.8 mg L^{-1} boron concentration levels for CuNP/CNT/GCE.

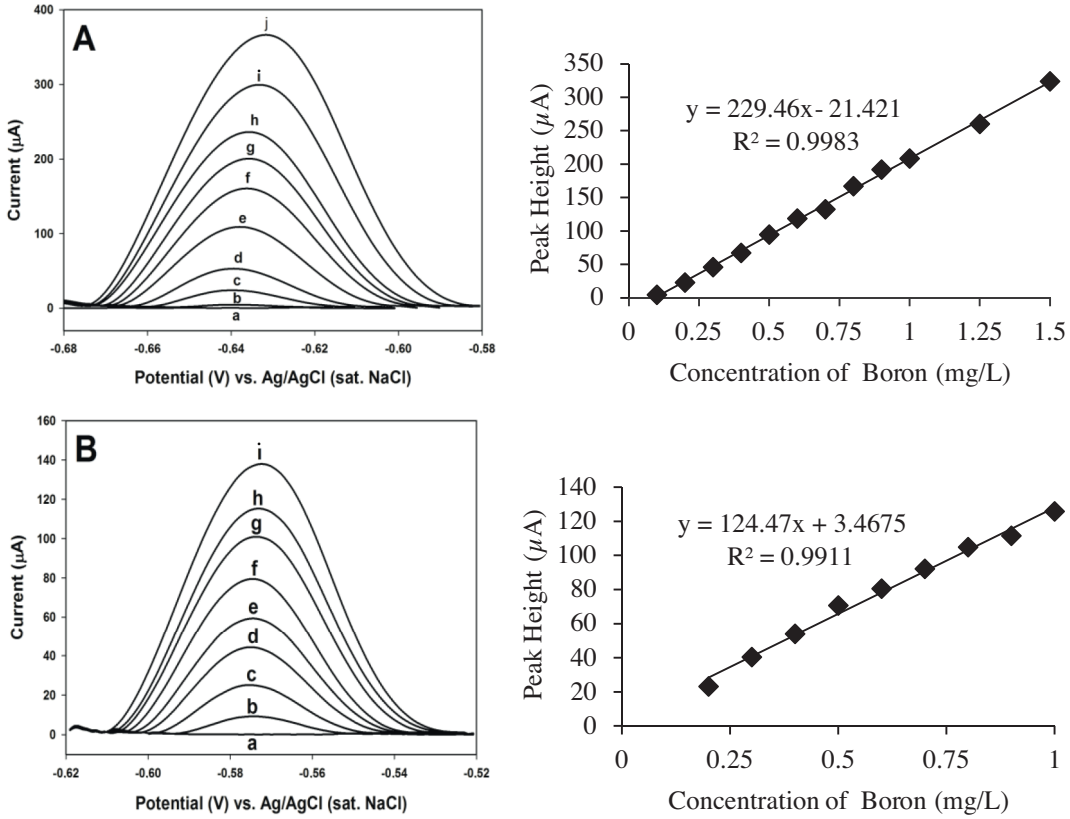

Figure 6. Voltammograms and calibration curves for various boron concentrations at AuNP/CNT/GCE (A): (a: 0.07 mM ARS + 0.5 M NH_4^+/NH_3 buffer, b: a + 200 μg L^{-1}, c: a + 300 μg L^{-1}, d: a + 400 μg L^{-1}, e: a + 500 μg L^{-1}, f: a + 600 μg L^{-1}, g: a + 800 μg L^{-1}, h: a + 1000 μg L^{-1}, i: a + 1250 μg L^{-1}, j: a + 1500 μg L^{-1}) and CuNP/CNT/GCE (B): (a: 0.07 mM ARS + 0.5 M NH_4^+/NH_3 buffer, b: a + 100 μg L^{-1}, c: a + 200 μg L^{-1}, d: a + 300 μg L^{-1}, e: a + 400 μg L^{-1}, f: a + 500 μg L^{-1}, g: a + 700 μg L^{-1}, h: a + 800 μg L^{-1}, i: a + 1000 μg L^{-1}).

The interference effects of Cl^-, NO_3^-, SO_4^{2-}, Na^+, K^+, Mg^{2+}, Ca^{2+}, Cu^{2+}, Cd^{2+}, Pb^{2+}, As^{3+}, Mo^{6+}, Mn^{2+}, Ni^{2+}, Cr^{3+}, Co^{2+}, Zn^{2+}, Se^{4+}, and Sb^{3+} ions were investigated in solution containing 1 mg L^{-1} of boron. The tolerable ratios were evaluated according to ±5% change in the peak height and calculated as 208 for Na^+; 45 for Cl^-; 25 for Mg^{2+}, NO_3^-, and SO_4^{2-}; 20 for Ca^{2+}; 15 for As^{3+}; 10 for Cd^{2+}, and K^+; 3 for Pb^{2+}; and 2 for Cu^{2+}, Mn^{2+}, Co^{2+}, Zn^{2+}, and Cr^{3+}. The results showed that Sb^{3+}, Mo^{6+}, Se^{4+}, and Ni^{2+} seriously interfered and decreased the peak height by about 24%, 16%, 8%, and 7%, respectively. The interferences except Sb^{3+} and Mo^{6+} were eliminated by the addition of 0.01 M ethylenediaminetetraacetic acid into the sample solution.

The method was applied to various water and eye drop samples. The results obtained are given in the Table. The recovery results changed between 97.2% and 103.5% for various water samples and eye drops for

both modified electrodes. The results obtained from the developed method for the two modified electrodes were compared separately with those obtained from the ICP-MS method and no statistically significant difference between the methods was found at the 95% confidence level. One-way ANOVA test results (last column in the Table) showed that there was no significant difference between the means of the three methods at 95% confidence level since the obtained experimental F values were smaller than the critical F value.

Additionally, a certified reference material (UME CRM 1201: Elements in Spring Water, Certificated Value = 0.481 ±0.023 mg L^{-1}) was used for the accuracy check of the proposed method. The means of seven independent measurement results were 0.480 ±0.024 mg L^{-1} for AuNP/CNT/GCE and 0.491 ±0.035 mg L^{-1} for CuNP/CNT/GCE. The results obtained were compared individually by using Student's t-test. The t-values calculated (1.62 for CuNP/CNT/GCE and 0.09 for AuNP/CNT/GCE) showed that there was no statistically significant difference between the means at 95% confidence level, indicating the good accuracy of the method (critical t value for N = 7 is 2.45).

2.5. Conclusions

A novel, sensitive, and accurate voltammetric method for determination of boron by using metal nanoparticle/carbon nanotube modified electrodes was described. The characterizations of the modified electrodes were made by CV, EIS, SEM, EDX, HRTEM, and XPS. MNP/CNT/GCEs were used for the first time for the voltammetric determination of boron. The peaks of the free ligand and boron-ligand complexes were well separated at both of the prepared electrodes. Compared with the CuNP/CNT/GCE, the AuNP/CNT/GCE has some advantages such as better repeatability, sensitivity, and wide analytical range. However, both modified electrodes illustrated good performance when studying samples containing 200 µg L^{-1} or more boron. The method can be recommended for determination of boron in tap water, drinking water, thermal water, and eye drop samples.

3. Experimental

3.1. Chemicals and equipment

Gold standard solution was obtained from Merck (for 1000 mg Au, $HAuCl_4.3H_2O$ in 12.7% HCl, Titrisol Gold Standard). MWCNT was supplied from Sigma Aldrich (>99%, O. D. × length: 6–13 nm × 2.5–20 µm) and used for electrode preparation. Other chemicals were used as analytical reagent grade. Ultrapure water (18.2 MΩ) was obtained from an ELGA brand PureLab Flex 2 model water purification system and the water was used for preparation of all solutions. All solutions were stored in high density polyethylene (HDPE) bottles.

Voltammetric measurements were performed using a Metrohm Autolab PGSTAT 128N with FRA32M Impedance Module connected to a BASi C3 cell stand and controlled by a PC. A three-electrode system consisting of gold or copper nanoparticles modified glassy carbon electrodes (BASi MF-2012, 3.0 mm diam.) as working electrodes, Ag/AgCl/3 M NaCl (BASi MF-2052 RE-5B with flexible connector) as reference electrode, and coiled platinum wire electrode (BASi MW-1033 (23 cm) with gold plated connector) as auxiliary electrode was used. pH measurements were made using a Mettler Toledo SevenEasy pH meter with combined pH electrode with temperature probe (MT-InLab Expert Pro) and temperature-controlled circulating bath (Thermo Haake DC 10 K20) for stable and accurate readings. An ISOLAB 3 L Ultrasonic Bath was used to clean the coiled platinum wire electrode and GCE.

Table. The results obtained from the proposed method using both modified electrodes and ICP-MS method for the determination of boron in real samples.

	Voltammetry AuNP/MWCNT/GCE			Voltammetry CuNP/MWCNT/GCE			ICP-MS			
Sample	B added ($mg\ L^{-1}$)	B found ($mg\ L^{-1}$)	R%	B added ($mg\ L^{-1}$)	B found ($mg\ L^{-1}$)	R%	B added ($mg\ L^{-1}$)	B found ($mg\ L^{-1}$)	R%	F [a]
Tap water	1	0.97 ±0.01	97.2	1	1.01 ±0.02	100.8	1	0.98 ±0.01	97.8	3.66
Drinking water	1	1.01 ±0.02	101.2	1	1.03 ±0.01	103.5	1	1.06 ±0.08	105.9	0.84
Thermal water	-	5.88 ±0.12	-	-	5.92 ±0.02	-	-	5.84 ±0.06	-	0.27
Eye drops [b]	-	2173.23 ±0.01	100.5	-	2162.25 ±0.01	100.0	-	2242.42 ±0.02	103.7	3.44

[a] Experimental F values (critical F value is 5.14).

[b] Specified boron content for eye drops is 2162.42 $mg\ L^{-1}$.

A JEOL JSM 6335-F model SEM with Aztec Energy Dispersive X-ray module was used for characterization of the used electrodes.

A JEOL 2100 high resolution transmission electron microscope and Thermo Fisher K-Alpha X-ray photoelectron spectroscopy were used for characterization of AuNP/CNT/GCE and CuNP/CNT/GCE.

3.2. Preparation of modified electrodes

MWCNT was weighed to 0.0392 g and transferred into a small beaker. Then 1.2 mL of concentrated H_2SO_4 and 0.4 mL of concentrated HNO_3 (3:1) were added to the beaker and boiled for 3 h at 90 °C, then washed many times with ultrapure water until obtaining a neutral supernatant. MWCNTs were dispersed in dimethylformamide (DMF) and ultrasonicated for 30 min.

The surface of the GCE was polished with 0.05 µm Al_2O_3 on synthetic cloth and rinsed with ultrapure water, then ultrasonicated in a 1:1 ethanol-ultrapure water mixture and ultrapure water, respectively. GCE was activated in ammonium/ammonia buffer solution (0.5 M pH 8.5) and 0.1 M KCl under 1.2 V for 120 s in stirring solution, and then potential was scanned from –1 V to 1 V with 50 mV s^{-1} scan rate until obtaining a stable background. The GCE surface was exposed to infrared light to evaporate the water. Then 10 µL of MWCNT suspension was dropped onto the GCE and exposed to infrared light for 5 min. This electrode was denoted as CNT/GCE and used for preparation of metal nanoparticle modified electrodes. The gold modification was performed in 5×10^{-5} M $HAuCl_4$ and 0.25 M H_2SO_4 solution using cyclic voltammetric potential scanning from 0.25 V to 1.30 V with 50 mV s^{-1} scan rate and 4 cycles. Copper modification was performed in 5×10^{-5} M $CuSO_4$ and 0.15 M H_2SO_4 solution using cyclic voltammetric potential scanning from –0.80 V to 0.70 V with 50 mV s^{-1} scan rate and 4 cycles. The modified electrodes were denoted as AuNP/CNT/GCE and CuNP/CNT/GCE, respectively.

3.3. Measurement procedure

Voltammetric measurements were applied in a quartz voltammetric cell. Before the measurements the GCE was activated and modified as mentioned beforehand. The solution containing ammonium/ammonia buffer (0.5 M pH 8.5), 0.1 M KCl, 0.07 mM ARS, and the required amount of boron was purged with argon gas for 5 min after the final volume was set to 10 mL. The instrumental parameters affecting the peak height such as step amplitude, interval time, pulse amplitude, pulse time, and accumulation potential and time were 1 mV, 0.275 s, 70 mV, 0.05 s, –900 mV, and 40 s, respectively. The working electrode was in the solution only during measurements and was washed before each measurement. All measurements were carried out at 21 ±3 °C.

3.4. Sample preparation procedure

Drinking water and tap water were collected from Gebze District of Kocaeli Province and thermal water was collected from Gönen District of Balıkesir Province in Turkey. Eye drops containing 2162.42 mg L^{-1} boron were purchased from a pharmacy in İstanbul. UME CRM 1201 (Elements in Spring Water) was obtained from the TÜBİTAK National Metrology Institute in Kocaeli, Turkey. The samples were stored in HDPE bottles at 21 ±3 °C. All samples were diluted with proper ratios.

Acknowledgments

This article is a part of the PhD thesis of Lokman Liv. This study was performed in the Electrochemistry Laboratory of TÜBİTAK UME. The authors would like to thank the Scientific Research Projects Division of Balıkesir University (Contract No: 2015/130) for the financial support.

References

1. Liv, L.; Nakiboğlu N., *Anal. Lett.* **2018**, *51*, 170-185.
2. Redondo-Nieto, M.; Pulido, L.; Reguera, M.; Bonilla, I.; Bolaños, L. *Plant Cell Environ.* **2007**, *30*, 1436-1443.
3. Liv, L.; Nakiboğlu, N. *Turk. J. Chem.* **2016**, *40*, 412-421.
4. US Environmental Protection Agency. *Drinking Water Health Advisory for Boron*; US Environmental Protection Agency: Washington, DC, USA, 2008.
5. World Health Organization. *Guidelines for Drinking Water Quality*; World Health Organization: Geneva, Switzerland, 2011.
6. Lewis, D. T. *Analyst* **1956**, *81*, 531-536.
7. Boyd, C. *Anal. Chem.* **1965**, *37*, 1587-1588.
8. Jin, W., Jiao, K., Metzner, H. *Electroanalysis* **1993**, *5*, 437-443.
9. Ünal, Ü.; Somer, G. *Electroanalysis* **2009**, *21*, 2234-2240.
10. Lu, G.; Li, X.; Deng, Y. *Food Chem.* **1994**, *50*, 91-93.
11. Thunus, L. *Anal. Chim. Acta* **1996**, *318*, 303-308.
12. Tanaka, T.; Nishu, K.; Nabekawa, H.; Hayashi, H. *ISIJ International* **2006**, *46*, 1318-1323.
13. Isbir, A. A. *Anal. Lett.* **2006**, *39*, 2835-2847.
14. Şahin, İ.; Nakiboğlu, N. *Fresen. Environ. Bull.* **2006**, *15*, 457-461.
15. Şahin, İ.; Nakiboğlu, N. *Anal. Chim. Acta* **2006**, *572*, 253-258.
16. Fujimori, T.; Akimoto, H.; Tsuji, Y.; Takehara, K.; Yoshimura, K. *Electroanalysis* **2010**, *22*, 1337-1343.
17. Tunay, Z.; Şahin, İ.; Nakiboglu, N. *Int. J. Electrochem. Sc.* **2011**, *6*, 6628-6638.